Water Content–Density Criteria for Determining Geomembrane–Fly Ash Interface Shear Strength

Katarzyna Zabielska-Adamska[1,*]

[1] Bialystok Technical University, Faculty of Civil and Environmental Engineering, Wiejska Street 45E, 15-351 Bialystok, Poland

Abstract. The aim of the present paper was to determine shear strength at the interface between fly ash, as a material underlying artificial sealing layer of storage yards, and HDPE geomembranes. The fly ash was compacted at moisture contents ranging over optimum water contents ± 5% using the standard Proctor test. The shear strength and interaction tests were conducted in classic direct shear apparatus with a cylindrical shear box. For interface strength tests the bottom box frame was equipped with a polycarbonate platen, which enabled geomembrane fixing. The shear strength of the interface contact of fly ash–smooth HDPE geomembrane did not greatly depend on moisture at compaction; however, it was important for textured geomembrane. The lowest interface strength was obtained at the highest moisture $w = w_{opt} + 5\%$, and the greatest values at moistures $w \geq w_{opt}$, for both geomembranes.

1 Introduction

Mineral soil liners and covers are most often single, double or multilayer complex sealing, consisting of compacted cohesive soil layers, with coefficient of permeability, k, lower than 10^{-9} m/s, characterised by a long-lasting ability to bond and interrupt movement of chemical compounds from landfill leachate as well as artificial layers – geomembranes [1-4]. Leakage through the damaged geomembrane is minimised by placing a mineral liner beneath the membrane [5-6]. In recent years, there has been much research on utilizing fly ash for mineral sealing layers, due to its chemical, physical and mechanical properties. The hydraulic conductivity of fly ash built-in mineral liners ranges from 10^{-6} to 10^{-9} m/s, and depends on fly ash compaction and calcium oxide content among other properties. Fly ash retains various contaminants including heavy metals [7-9]. Fly ash water-permeability decreases with time, and using waste leachate for permeability tests does not affect or slightly decreases it [8, 10]. Fly ash hydraulic conductivity remained constant after adding alkaline or neutral non-organic solution, and increased with acidity [9, 11]. Shear strength of compacted fly ash and its bearing capacity are significantly greater than for mineral soils of similar grain size, at similar values of consolidation [12, 13].

In the present study the shear strength interface between compacted fly ash, as a material underlying artificial sealing layers of storage yards, and HDPE geomembranes with smooth or textured textures, is shown. In previous research it has been frequent practice to present the shear strength values of interface contact only for mineral soil compacted at water content closed to optimum. The permeability and mechanical properties of compacted non-cohesive fly ash and fly ash/bottom ash mixture are dependent on moisture content during compaction, w, as are properties of cohesive mineral soils [14]. Consequently, different values are obtained for w on either side of the w_{opt} on a compaction curve, for the same dry densities, ρ_d. Thus, w at compaction would be expected to affect interface shear strength. The aim of the present study was to identify the dependence of interface contact parameters on fly ash moisture content at compaction. The tested fly ash was compacted by the Standard (SP) Proctor method at various w ranging over $w_{opt} \pm 5\%$, with reference to specific fly ash properties.

2 Background

Interface contact is most often tested in modified direct shear apparatus or torsional-ring shear apparatus. For interface shear strength the generalised classic Coulomb condition assumes the form:

$$\tau_f = \sigma \cdot \tan\delta + c_a \qquad (1)$$

where τ_f is the soil–geomembrane contact resistance at the moment of shearing, σ the shear stress to destruction plane (normal stress), c_a the adhesion and δ the interface friction angle.

Shear strength test results of soil–geomembrane contact are usually presented for the peak strength (maximum contact resistance at the moment of shearing) and residual strength (steady-state value of shearing resistance). In order to reach the steady-state, a large shear displacement may be required, so a torsional-ring shear apparatus or shear box larger than used in classic tests is necessary. It is considered that test results of the

* Corresponding author: kadamska@pb.edu.pl

interface shear strength, presented as peak values at maximal shearing resistance, should be used in stability analysis of waste disposal site base. Residual strength values (at a steady-state) are applied when calculations of surface sealing layer stability are done for the sake of predicted displacement values in multi-layer sealing [15].

Dove et al. [16] tested dependence of non-cohesive soil particle shape on speed of mobilising peak values or reaching steady state of shear strength for non-dilative interface systems. The displacement requirement to reach a steady state decreased as particle angularity increased, but peak values were obtained more slowly. They concluded that rounded and sub-rounded grains may need a large-displacement shearing test to reach a steady state. Concluding with these statements to present study, spherical fly ash grains may require less time for peak value mobilization than mineral soil grains. A steady state should be reached quickly, as highly brittle fly ash grains are damaged in the process and become more angular during shearing and interface shearing.

The dependence between interface contact parameters and *w* of mineral clay layers at compaction was found in tests after slope-stability failure in hazardous waste landfill at the Kettleman Hills [17]. Seed and Boulanger [18] attempted to determine interface shear strength, between a compacted clay mineral layer and a smooth HDPE geomembrane, depending on moisture content at compaction by the SP method. Tests were carried out in direct shear apparatus with a small box, under unconsolidated and undrained conditions. They found that interface shear strength decreased with increased moisture content at compaction. Differences in strength values versus moisture content were reduced when samples were pre-soaked under light surcharge before shearing. On the basis of tests by other researchers, Stark and Poeppel [15] described the impact of clay water content at compaction on interface strength, which decreased with increased normal stress, nearly completely disappearing at σ = 48 kPa, for peak as well as residual values. Interesting tests on clay soils or Ottawa sand contact with smooth geomembranes were done in modified direct shear apparatus, fitted with a miniature pore pressure transducer to measure pore-pressure changes close to soil–geomembrane contact [19, 20]. Soil samples were compacted at various *w* to the same bulk density and tested under saturated and unsaturated conditions. They reported that the suction nearby the geomembrane surface took part in the mobilisation of interface shear strength and caused effective normal stresses to be higher than total normal stresses, increasing interface shear strength values in the low normal stress range. The shear-strength equation for unsaturated soils was satisfactory used for describing interface shear strength at normal stresses lower than 20 kPa.

3 Laboratory tests

3.1 The materials

Laboratory tests were performed on samples of power industry waste from bituminous coal combustion in Thermal-Electric Power Station in Bialystok (Poland), stored in a dry storage yard. This waste is referred to as *fly ash* since it had only a vestige of bottom ash. Fly ash, regardless of origin, is fundamentally aluminosilicate glass and may consist of clay minerals mullite or kaolinite, among others. Scanning electron micrograph (SEM) images of fly ash particles (Fig. 1) show a complex structure of different glassy spheres, spheroids and agglomerates.

a)

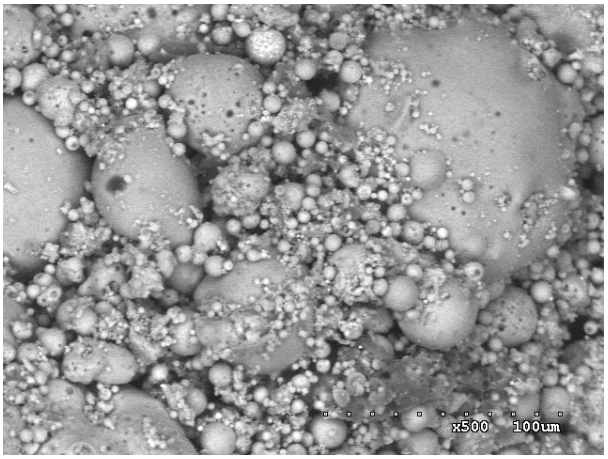

b)

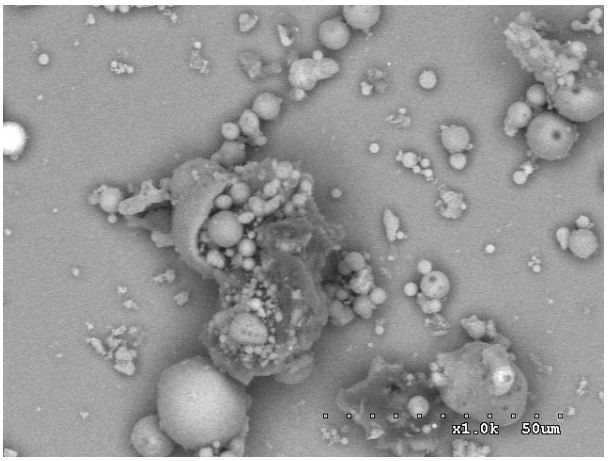

Fig. 1. Scanning electron micrographs (SEM): (a) a general view of tested fly ash grains with visible smooth and vesicular aluminosilicate cenospheres and (b) some crumbled (after compaction) fly ash grains.

All tests were carried out on the same fly ash shipment, which graining was similar to sandy silt. The median diameter D_{50} was 0.07 mm. The uniformity coefficient, C_U, equalled 4.00 rated it as a uniform soil (uni-fraction). The curvature coefficient, C_C = 1.26, indicated fly ash was relatively well graded for compaction. The average density of solid particles was very low about 2.09 ± 0.03 Mg/m^3. Compaction parameters were obtained by means of the SP method, thus each point of the compaction curve was determined for separately prepared specimen. Fly ash re-compaction

causes partial crumbling of dynamically rammed grains and changes physical properties, giving incorrect estimation of compaction effects. During compaction, smaller grains stuff greater spherical (empty) grains that have been partly crushed, so fly ash dry density and compaction are better [21]. The maximum dry density, $\rho_{d\ max}$, was 0.984 Mg/m^3 and optimum water contents, w_{opt}, 46.0% by the SP method.

Shear strength tests were performed in direct shear apparatus, under the same conditions as interface contact tests, on fly ash compacted at the range w_{opt} ± 5% (Fig. 2). Fly ash internal friction angle, ϕ, decreased along with increased moisture content at compaction ranged: ϕ = 38.5–41.9°. Fly ash cohesion resistance was clearly affected by w, with the highest values at w_{opt}, being similar to compaction curve shapes. The cohesion resistance, c, was 42.8–69.7 kPa. Residual strength parameters were: ϕ_{res} = 32.9–35.0°, c_{res} = 22.9–36.6 kPa.

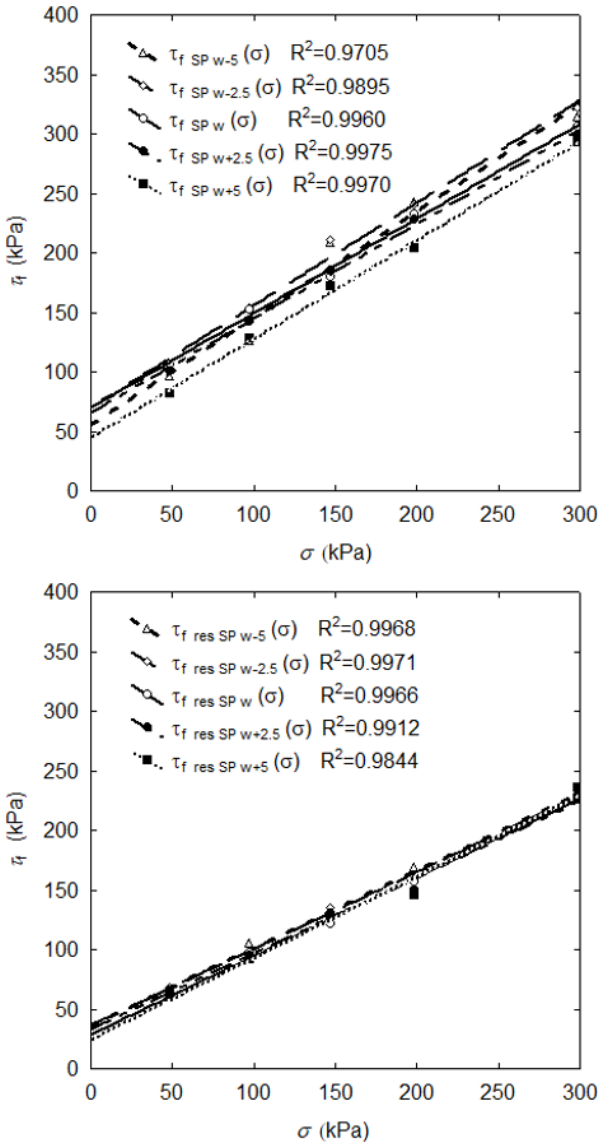

Fig. 2. Shear strength of fly ash alone compacted at moisture contents w_{opt} ± 5%: $\tau_{f\ SP}(\sigma)$ – peak strength, $\tau_{f\ res\ SP}(\sigma)$ – residual strength.

Two HDPE geomembranes, one smooth and one textured, were used in the tests, both with a core thickness of 1.5 mm. The textured geomembrane roughness (Fig. 3), co-extruded during manufacture, had an average height on the outside surface of 0.5 mm (point convexities irregularly placed on the surface 0.5–4 mm apart).

Fig. 3. The tested HDPE textured geomembranes.

3.2 The interface test method

ASTM D 5321 [22] describes minimum box dimensions, dependent on soil grain size, as greater than 15 times the D_{85}. In tested fly ash, the effective size D_{85} = 0.15 mm, so conventional direct shear apparatus of 10x10 cm or even 6x6 cm is adequate for tests. Considering HDPE geomembrane hardness and uniform surface tested geomembranes, it has been concluded that a small box may be used [23, 24].

Fly ash shear strength and interaction tests between HDPE geomembrane and compacted fly ash were conducted in classic direct shear apparatus with a cylindrical shear box. The box (65 mm inner diameter, 20 mm high) enables testing of compacted soil. For interface strength tests the bottom box frame was equipped with a polycarbonate (PC) platen, which enabled geomembrane fixing [12]. The HDPE geomembrane was cut to 9.0 cm in diameter and glued on the upper surface of the PC platen placed in the bottom box frame. The diameter of the PC platen was 25 mm greater than the upper box frame, to keep constant surface of interface contact during the shearing test. The upper box frame was put on the PC platen and the whole box bolt-clipped. Fly ash specimens were compacted in a bipartite device, designed for forming of non-cohesive soil sample, and carefully relocated to upper box frame and covered by porous stone and load head.

Fly ash was compacted at five different w in the range w_{opt} ± 5%, for SP method, reaching dry densities corresponding to compaction curves. Undrained samples were sheared at normal stresses of 50, 100, 150, 200 and 300 kPa, with a displacement rate of 1 mm/min (1.67x10^{-4} m/s), without soaking the samples in water. Relatively small values of pore-water pressure were obtained during shearing, so this displacement rate could be applied [25]. The test readings were automatically logged by a computerised system.

3.3 The test results

The fly ash–geomembrane interface strength test results in reference to displacement in direct shear apparatus for smooth geomembrane are shown in Fig. 4, and for textured geomembrane in Fig. 5.

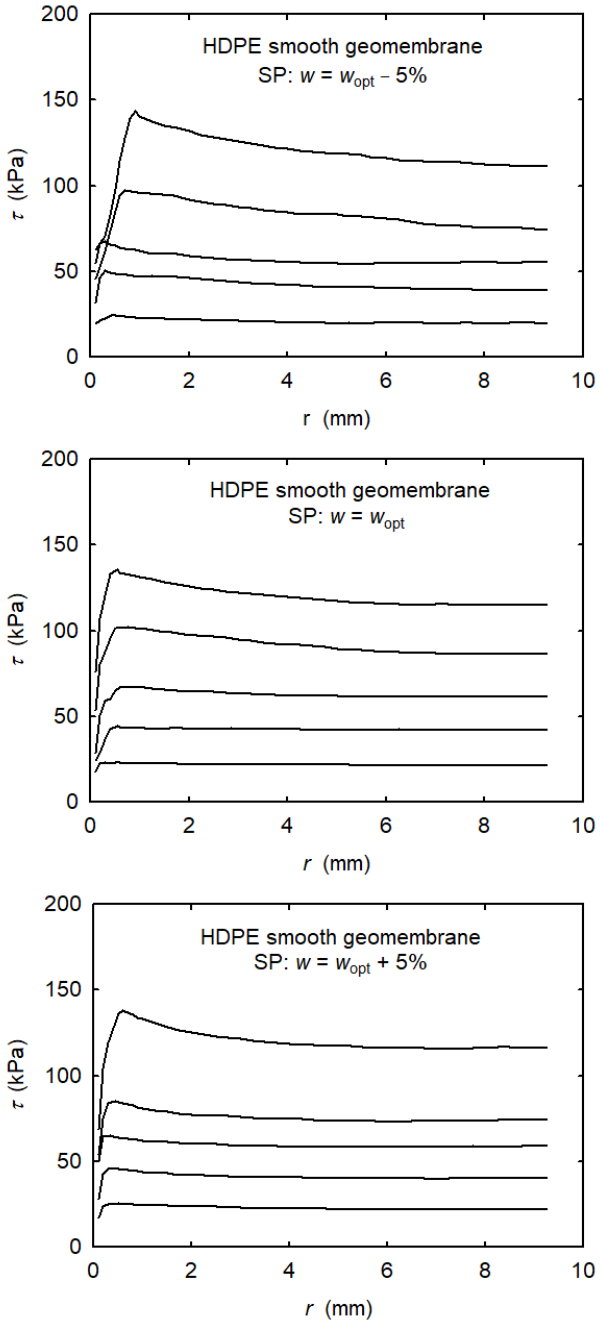

Fig. 4. Fly ash–smooth HDPE geomembrane shearing resistance stress in dependence on sample displacement, *r*, tested at values of normal stress σ equalled 50, 100, 150, 200 and 300 kPa, for moisture contents at compaction $w_{opt} \pm 5\%$.

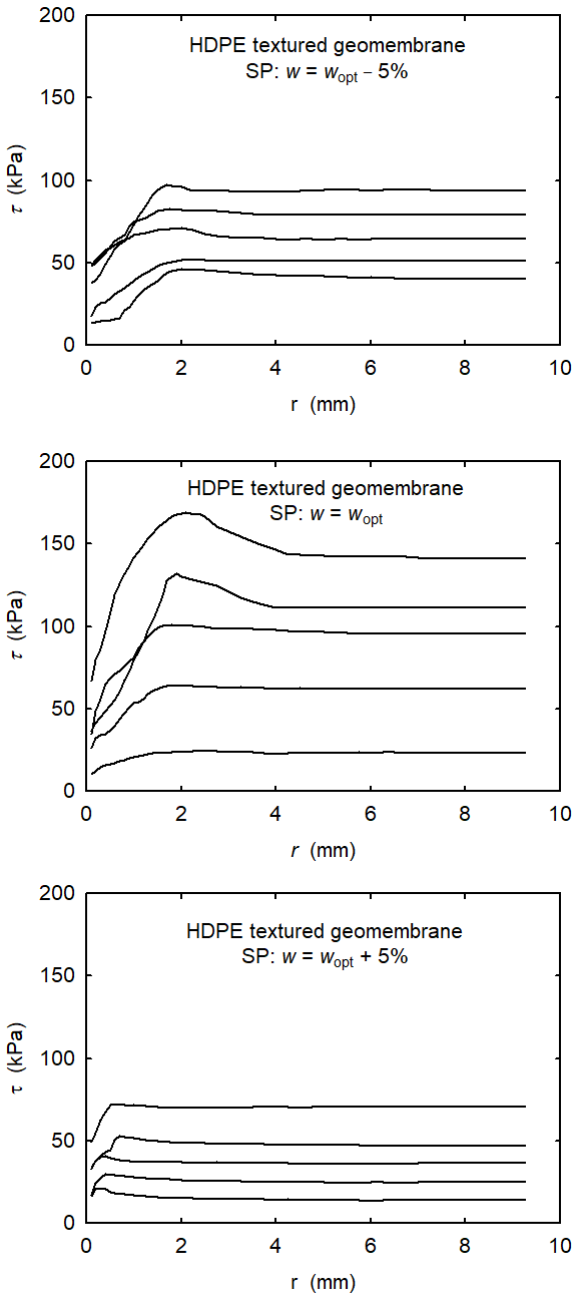

Fig. 5. Fly ash–textured HDPE geomembrane shearing resistance in dependence on sample displacement, *r*, tested at values of normal stress σ equalled 50, 100, 150, 200 and 300 kPa, for moisture contents at compaction $w_{opt} \pm 5\%$.

The more diverse geomembrane texture is, the greater displacement is achieved for mobilised peak strength. For smooth geomembrane and fly ash compacted by SP method the peak strength was reached at 0.5–1.0 mm displacement. In textured geomembrane, peak strength of SP compacted fly ash was mobilised at 0.75–2.0 mm displacement. Fly ash moisture content influenced speed of mobilisation of peak values of the interface contact strength. The higher the fly ash *w*, the faster the peak value was achieved in interface contact shearing tests, independently of geomembrane texture.

In all the cases, after reaching the peak the contact strength reduction to the set value of shearing resistance took place, reached in most tests at a displacement of about 6 mm, and determined approximately 10% of the tested fly ash sample diameter. Further in the paper this set strength will be called the residual strength although the residual values obtained during large displacement were not checked out.

4 Discussion

4.1 Interface contact shear strength

Fly ash moisture had little effect on interface shear strength for smooth geomembranes. Interface peak strengths were similar for all moisture contents. However, in all tests when $w = w_{opt} + 5\%$ at compaction, the contact strength was reduced in comparison to lower moisture content (Fig. 6). Shear strengths were more affected by water content ($w = w_{opt} \pm 5\%$) at compaction, for textured geomembranes. The curves of shear strength versus displacement indicated the effect of moisture at compaction on interface contact quality (Fig. 5). Various interface shear strengths were obtained at particular w values but when $w > w_{opt}$, the shape of stress-displacement curves changed significantly. The greater importance has the fly ash compaction effort in comparison to smooth geomembrane. It did not much affect the interface strength value only at optimum water contents. The lowest interface strength values (at σ = 300 kPa) were at w_{opt} + 5%, similarly to fly as shearing. The highest interface strength was at w_{opt} (Fig. 7), for interface shear strength, peak and residual values.

The non-linear $\tau_f = f(\sigma)$ relationships were observed, similarly to other researchers [23, 26-27], but generally for textured geomembrane (Fig. 8). Fitting curvilinear relationships were not attempted since linear relationships were statistically significant. Determination coefficients for linear relationships for peak and residual values ranged: 0.9683–0.9623 and 0.9999–9272, respectively.

The distinct rise of shear strength values for textured compared to smooth geomembrane was not observed. There were greater shear strengths for textured geomembrane for SP method (peak and residual values) only at w_{opt}. The interface friction angle, δ, for fly ash–textured geomembrane was about 5° greater than for smooth geomembrane, when fly ash was compacted at w_{opt}. This difference was reduced as moisture content at compaction increased, and when $w = w_{opt} + 5\%$, δ was greater for smooth geomembrane. When $w < w_{opt}$ there was the greatest adhesion in textured geomembrane; however, for smooth geomembrane adhesion remained nearly constant at all w. The interface strength parameters, c_a and δ (Table 1), changed greatly over $w_{opt} \pm 5\%$ for textured geomembrane, but for smooth geomembrane were similar across w values.

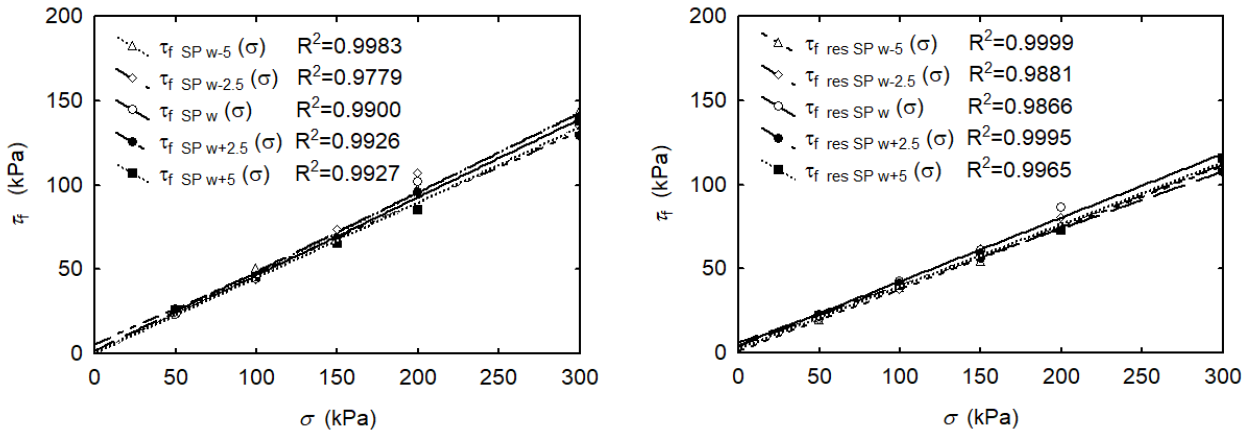

Fig. 6. Shear strength of fly ash–smooth HDPE geomembrane contact, for fly ash compacted at moisture contents $w_{opt} \pm 5\%$: $\tau_{f\,SP}(\sigma)$ – peak strength, $\tau_{f\,res\,SP}(\sigma)$ – residual strength.

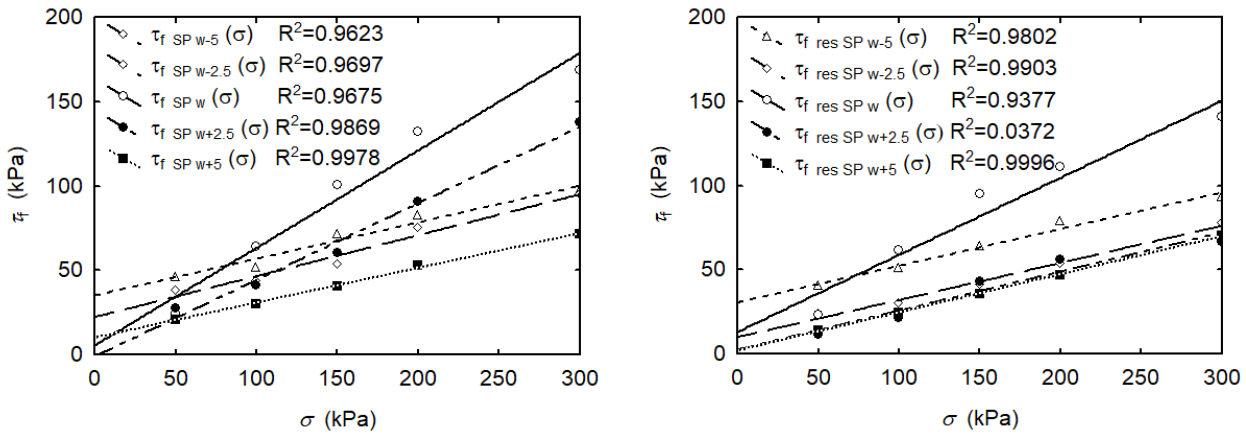

Fig. 7. Shear strength of fly ash–textured HDPE geomembrane contact, for fly ash compacted at moisture contents $w_{opt} \pm 5\%$: $\tau_{fSP}(\sigma)$ – peak strength, $\tau_{f\,res\,SP}(\sigma)$ – residual strength.

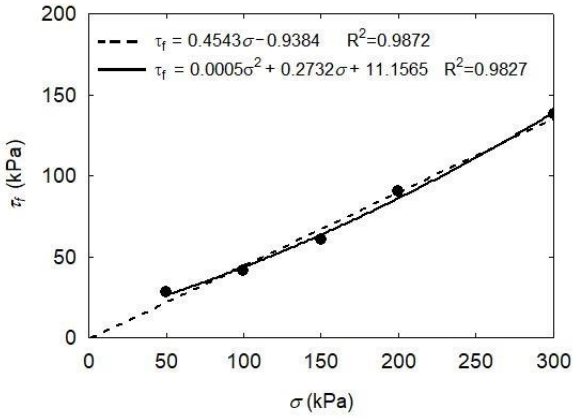

Fig. 8. Shear strength of fly ash–textured HDPE geomembrane contact with linear and curvilinear fitting (fly ash compacted at $w = w_{opt} + 2.5\%$).

Table 1. The ranges of interface contact parameters for fly ash SP compaction method and various geomembrane texture.

Texture	Interface contact parameter			
	δ (deg.)	δ_{res} (deg.)	c_a (kPa)	$c_{a\,res}$ (kPa)
Smooth	25.6–22.9	20.8–18.8	5.7–0	6.1–0.9
Textured	29.7–11.7	24.4–12.4	35.3–0	30.7–1.9

Explanation: Negative values of adhesion are replaced with null values.

In some tests there were negative values of adhesion, representing a mathematic quantity from linear approximations of limited states, and not a true physical value. Fleming et al. [19] justified negative adhesion values as a result of bilinear curve of interface shear strength $\tau_f = f(\sigma')$, estimated for effective normal stresses. There were caused by change of shear failure mechanism from sliding to combined sliding and ploughing at higher normal stress, which was explained by soil particles embedding into the smooth geomembrane.

In the present study, negative adhesion values were more often for smooth geomembrane (Fig. 1). Statement about other interface failure mechanism may be legitimate, though obtained negative values were very little. Scratches were observed on the smooth geomembrane surface, thus fly ash grain ploughing had occurred. Due to the fragility of fly ash grains they have less capacity to plough than sandy soils mainly made of quartz [28]. Generalising, apart from quartz (SiO_2), tested fly ash consists of mullite ($Al_6Si_2O_{13}$) and calcite ($CaCO_3$).

4.2 Fly ash shear strength

The maximum peak shear strength values (Fig. 2) were at $w < w_{opt}$ and minimum values at $w = w_{opt} + 5\%$. Curves $\tau_f = f(\sigma)$, determined for set values, practically agree with each other, so w at compaction did not influence residual shear strength. In the tested moisture content range there were nearly constant values of residual internal friction angle, ϕ_{res}; the residual cohesion resistance, c_{res}, decreased with increased w.

Comparable relationships between peak values of clay shear strength parameters for non-saturated clay, compacted by SP method at various w, above and below w_{opt}, were described by Cokca et al. [29]. There was a bilinear relationship between ϕ and w at compaction. The soil suction linearly increased as w decreased on the dry side of optimum to value of optimum water content. Next, soil suction decreased slightly with increased w. Generalizing, as w increased the soil suction values decreased, so greater suction generated higher values of ϕ. They also found maximum cohesion at around clay w_{opt}.

Summarising, cohesion reduced with decreased w on the dry side of w_{opt} of compacted unsaturated clay, which was caused by the granular character of clay at low degrees of saturation. On the wet side cohesion decreased with w as clay particles became hydrated and increased in size, surrounded by a thin water film. Macroscopic non-cohesive fly ash, with spherical grains, after compaction at various w of range $w_{opt} \pm 5\%$, has a similar shear strength relationship versus w at compaction as non-saturated clay. This interesting result is despite obtaining relatively small values of pore-water pressure during shearing.

Generalising, interface shear strength between fly ash compacted by SP method at the range $w_{opt} \pm 5\%$ and HDPE geomembranes (smooth or textured) is dependent on moisture content at compaction. The lowest values of contact strength were obtained at $w = w_{opt} + 5\%$, similar to results for fly ash alone. Results of the present paper may be due to easier sliding between fly ash grains or at the grain–geomembrane surface from water films surrounding grains, and also between grains and the geomembrane, and the softening of grains by high moisture content. Softer fly ash grains would contribute to the lowest friction coefficient at the interface. The highest friction values at $w \leq w_{opt}$ (in nearly all tests) were probably caused by the densest packing of fly ash grains or greater fly ash shear strength, which is significant for textured geomembrane. Differences in interface strength reduced with decreased σ. At σ = 50 kPa, for smooth geomembrane, shear strength values were the same, and for textured geomembrane the differences were the smallest. Fly ash moisture content at compaction affects the speed of mobilisation the peak values of interface shear strength. The greater fly ash w at compaction, the quicker was the peak value mobilisation of interface shear strength reached.

The shear strength of fly ash–HDPE geomembrane contact was less than that of fly ash alone for all cases tested at normal stress ranges (50–300 kPa), which was different to clay test results [30].

Quality and stability of geoemembrane texture have a significant impact on shear strength of interface contact. Texture destruction was observed in laboratory tests on the textured geomembrane, while peak values of interface contact strength were at set values. In present study these results were not shown. Greater dependence on texture has been found in geomembrane with more diverse texture [12]. In laboratory tests of interface shear strength between fly ash compacted at w_{opt} and HDPE

geomembranes with distinct and stable texture, shear strength of nearly twice the size were obtained (at σ = 300 kPa), in comparison to smooth geomembrane. Poor geomembrane texture changes the interface shearing mechanism, so instead of mainly internal shearing there is slippage at the interface, which deteriorates interface contact.

5 Conclusions

The shear strength values of the interface of fly ash–smooth HDPE geomembrane do not greatly depend on fly ash moisture content. Approximately the same values of interface peak strength were obtained for all moisture contents. However, the minimum interface shear strengths were at the highest moisture contents (w_{opt} + 5%) and the maximum values at $w \leq w_{opt}$. Moisture content at compaction had more visible influence for textured geomembrane. The minimum values were also obtained at the highest moisture content and the maximum values – at optimum water content.

Minimal values of interface shear strength are obtained at the highest degree of saturation ($w = w_{opt}$ + 5%), when fly ash grains were softer and more slippery due to a water film. At greater saturation pore water causes sliding between fly ash grains and between grains and the geomembrane. At lower w the increased fly ash suction values may generate higher ϕ between grains and also at the interface contact.

Interface shear strength did not always decrease with increased w at compaction as for clay–smooth geomembrane [15, 18], but it may reach a maximum at fly ash w_{opt} and difference increased along with increased normal stress. When interface shear strength is determined only at w_{opt}, it is necessary to consider that it may be significantly decreased at other values of w.

In engineering practice, construction of mineral sealing layers usually requires soil compaction at a determined moisture range to obtain 90 or 95% of maximum compaction, relating to SP method. Care should be taken not to use compaction degree (% of maximum compaction) as the only parameter to assess compaction of material in a sealing layer. This applies to both cohesive soil and to fly ash.

The work, carried out at Bialystok Technical University in Poland, was supported by Polish financial resources on science under project numbers 5 T07E 051 24 and S/WBiIS/2/2018.

References

1. D.E. Daniel, *Geotechnical Practice for Waste Disposal*, Chapman & Hall, London, England, 683 pp. (1997)
2. R.K. Rowe, Long-term performance of contaminant barrier systems, Geotechnique **55**, 631–678 (2005)
3. R.K. Rowe, R.M. Quigley, R.W.I. Brachman, J.R. Booker, *Barrier Systems for Waste Disposal Facilities*, Taylor & Francis Books Ltd. (E & FN Spon), London, England, 400 pp. (2004)
4. W. F. Van Impe, Environmental Geotechnics: ITC 5 activities. State of the art. In: *Environmental Geotechnics*, Seco e Pinto (Ed.), A.A. Balkema, Rotterdam, pp. 121–126 (1998)
5. R.W.I. Brachman, A. Sabir, Geomembrane puncture and strains from stones in an underlying clay layer. Geotext. Geomembranes **28**, 335–343 (2010)
6. Q. Xue, Q. Zhang, Z.-Z. Li, K. Xiao, The tension and puncture properties of HDPE geomembrane under the corrosion of leachate. Materials **6**, 4109–4121 (2013)
7. D. Dertmatas, X. Meng, Utilization of fly ash for stabilization/sodification of heavy metal contaminated soils, Eng. Geol. **70**, 377–394 (2003)
8. T.B. Edil, L.K. Sandstrom, P.M. Berthoux, Interaction of inorganic leachate with compacted pozzolanic fly ash, J. Geotech. Geoenviron. Eng. **118**, 1410–1430 (1992)
9. C.T. Nhan, J.W. Graydon, D.W. Kirk, Utilizing coal fly ash as a landfill barrier material, Waste Manage. **16**, 587–595 (1996)
10. M.M. Leppänen, A. Kaartokallio, E. Loukola, Full scale landfill bottom liner test structures at Ämmäaauo Landfill, Espoo, Finland. In: *Proceedings of the 7th International Waste Management and Landfill Symposium*, Sardinia, Italy (1999)
11. P.V. Sivapullaiah, H. Lakshmikantha, Properties of fly ash as hydraulic barrier, Soil. Sediment. Contam. **13**, 489–504 (2004)
12. K. Zabielska-Adamska, Shear strength parameters of compacted fly ash–HDPE geomembrane interfaces, Geotext. Geomembranes **24**, 91–102 (2006)
13. K. Zabielska-Adamska, M.J. Sulewska, Dynamic CBR test to assess the soil compaction, J. Test. Eval. **53**,1028–1036 (2015)
14. K. Zabielska-Adamska, One-dimensional compression and swelling of compacted fly ash. Geotech.Res. https://doi.org/10.1680/jgere.17.00017 (2018)
15. T.D. Stark, A.R. Poeppel, Landfill liner interface strengths from torsional–ring–shear tests, J. Geotech. Eng. **120**, 597–615 (1994)
16. J.E. Dove, D.D. Bents, J. Wang, B. Gao, Particle scale surface interaction of non-dilative interface systems, Geotext. Geomembranes **24**, 156–168 (2006)
17. J.K. Mitchell, Geotechnical surprises – Or are they? J. Geotech. Geoenviron. Eng. **135**, 998–1010 (2009)
18. R.B. Seed, R.W. Boulanger, Smooth HDPE–clay liner interface shear strength: compaction effect, J. Geotech. Eng. **117**, 686–693 (1991)
19. I.R. Fleming, J.S. Sharma, M.B. Jogi, Shear strength of geomembrane–soil interface under unsaturated conditions, Geotext. Geomembranes **24**, 274–284 (2006)

20. J.S. Sharma, I.R. Fleming, M.B. Jogi, Measurement of unsaturated soil–geomembrane interface shear parameters, Can. Geotech. J. **44**, 78–88 (2007)
21. K. Zabielska-Adamska, Laboratory compaction of fly ash and fly ash with cement additions, J. Hazard. Mater. **151**, 481–489 (2008)
22. ASTM Standards: D 5321, *Standard test method for determining the coefficient of soil and geosynthetic or geosynthetic and geosynthetic friction by the direct shear method*, ASTM International, West Conshohocken, PA, USA (2017)
23. H.I. Ling, A. Pamuk, M. Dechasakulsom, Y. Mohri, Ch. Burkr, Interactions between PVC geomembranes and compacted clay, J. Geotech. Geoenviron. Eng. **127**, 950–954 (2001)
24. T.D. O'Rourke, S.J. Druschel, A.N. Netravali, Shear strength characteristic of sand–polymer interfaces, J. Geotech. Eng. **116**, 451–469 (1990)
25. Ch. Hsieh, M.-W. Hsieh, Load plate rigidity and scale effects on the frictional behaviour of sand/geomembrane interfaces, Geotext. Geomembranes **21**, 25–47 (2003)
26. J. J. B. Esterhuizen, G. M. Filz, J. M. Duncan, Constitutive behaviour of geosynthetic interfaces, J. Geotech. Geoenviron. Eng. **127**, 834–840 (2001)
27. J.P. Giroud, J. Darrasse, R.C. Bachus, Hyperbolic expression for soil-geosynthetic or geosynthetic-geosynthetic interface shear strength, Geotext. Geomembranes **12**, 275–286 (1993)
28. P. Punetha, P. Mohanty, M. Samanta, Microstructural investigation on mechanical behavior of soil-geosynthetic interface in direct shear test, Geotext. Geomembranes **45**, 197–210 (2017)
29. E. Cokca, O. Erol, F. Armangil, Effect of compaction moisture content on the shear strength of an unsaturated clay, Geotech. Geol. Eng. **22**, 285–297 (2004)
30. K.L. Fishman, S. Pal, Further study of geomembrane/cohesive soil interface shear behaviour, Geotext. Geomembranes **13**, 571–590 (1994)